1st Faculty of Medicine, Department of Paediatrics
Charles University, Prague, Czech Republic

HEMOPROTEIN NITRIC OXIDE SYNTHASE IN *APLYSIA CALIFORNICA*

PhD thesis summary

MUDr. Michaela Buganová

Prague 2008

This PhD Thesis was elaborated during Postgraduate Studies in Biomedicine at the Laboratory for Study of Mitochondrial Disorders of the Department of Paediatrics, 1st Faculty of Medicine, Charles University, Prague, Czech Republic.

Commission: Biochemistry and Pathobiochemistry

Chairman of the Commission for Biochemistry and Pathobiochemistry:
Prof. MUDr. Jiří Kraml, DrSc.
Department of Clinical Biochemistry and Laboratory Medicine
1st Faculty of Medicine, Charles University
Kateřinská 32, 121 08 Prague 2

Author: MUDr. Michaela Buganová

Address: Laboratory for the Study of Mitochondrial Disorders
Department of Paediatrics
1st Faculty of Medicine, Charles University
Ke Karlovu 2, 128 08 Prague 2
Tel/fax: 224910478
Email: mbod@email.cz

Supervisor: Prof. MUDr. Pavel Martásek, PhD.
Department of Paediatrics,
Ke Karlovu 2, 128 08, Prague 2

Opponents: Prof. RNDr. Václav Pelouch, CSc.
Department of Medical Chemistry and Biochemistry
2nd Faculty of Medicine, Charles University
Plzeňská 221/130, 150 06 Prague 5

Prof. MUDr. Rastislav Druga, DrSc.
Department of Anatomy
2nd Faculty of Medicine, Charles University
U nemocnice 3 , Prague 2, 128 00

Date of Defence of PhD Thesis: 19th of June, 2008

Place of Defence: Charles University, Prague, Czech Republic

The thesis is available and is placed at the 1st Faculty of Medicine, Charles University, Kateřinská 32, 121 08 Prague 2.

CONTENTS

ABSTRAKT ČESKY (ABSTRACT IN CZECH)

Oxid dusnatý (NO) má nezastupitelnou roli v neuronální signalizaci v řadě eukaryotických a prokaryotických organizmů. NO-syntázy (NOS) jsou hem-obsahující monooxygenázy, které v přítomnosti kyslíku katalyzují oxidaci L-argininu na NO a L-citrulin. NO produkovaný NO-syntázou je plynná molekula, která lehce difunduje přes membrány a zprostředkovává jak mezibuněčnou, tak i vnitrobuněčnou komunikaci. NO aktivuje enzymy vážící kovy včetně solubilní guanylátcyklázy (sGC), a tím zvyšuje hladinu druhého posla cyklického guanosinmonofosfátu (cGMP) (1, 2), který dále zprostředkovává řadu fyziologických a patologických procesů v neuronech. Nicméně, detailní charakteristika nitrergních neuronů a funkce NO v centrální nervové soustavě (CNS) není zcela objasněna.

Cílem dizertační práce bylo charakterizovat neuronální NOS, proteiny spojené s metabolismem neuronální NOS a signální dráhu NO v CNS zeje kalifornského (*Aplysia californica*), populárního experimentálního modelu buněčných a systémových neurověd.

Na biochemické úrovni byla zjištěná závislost NOS *Aplysie* (*Ac*NOS) na kalciu- kalmodulinu (Ca-CaM) a NADPH. Řada reprezentativních inhibitorů savčích NOS isoforem též snížila NOS aktivitu u *Aplysie*. Polyklonální protilátky vytvořené proti krysí NOS hybridizovaly na Western blotu s purifikovanou *Ac*NOS (160 kDa protein) z částečně purifikovaných CNS homogenátů.

Aktivita *Ac*NOS popsaná v této práci byla asi šestkrát nižší než zjištěná aktivita NOS v savčím mozečku (3), ale aktivita *Ac*NOS byla srovnatelná s průměrnými hodnotami uváděnými pro nervovou soustavu hmyzu (4, 5). Stanovili jsme bazální hodnoty produkce cGMP v CNS *Aplysie*. Stimulace NOS donory NO nebo inkubace s inhibitory fosfodiesterázy významně zvýšily hodnoty cGMP. Specifický inhibitor sGC snížil bazální hodnoty cGMP o polovinu a předešel zvýšení cGMP za přítomnosti NO. Na základě těchto výsledků lze předpokládat, že NO funguje jako posel v CNS *Aplysie* a že cGMP je jedním z efektorů NO.

Klonovali jsme *Ac*NOS v jeho plné délce a dokumentovali, že obsahuje všechny konzervované části charakteristické pro funkční NOS u obratlovců. Lokalizovali a zmapovali jsme nitrergní neurony v CNS *Aplysie*. Pomocí *in situ* hybridizace a imunohistochemicky byla prokázána přítomnost NOS v přibližně 2% všech centrálních neuronů.

Optimalizovali jsme protokol pro vícebarevnou *in situ* hybridizaci s použitím celých ganglií („whole mount"), tedy bez nutnosti připravovat řezy. S využitím této nově zavedené metody jsme identifikovali neurony, ve kterých jsme následně korelovali jejich proteinová expresní data a jejich funkci. Tím jsme sestavili i úplnou topografickou mapu uspořádání mechanosensorických neuronů v CNS *Aplysie* exprimujících neuropeptid sensorin-A.

Hodnotili jsme působení jednostranného mechanického poškození „nožního" nervu na úroveň exprese NOS mRNA v neuronech „nožního" ganglia v souvislosti s funkčním významem NO v regeneraci nervů a u neuropatických bolestí. Výsledky *in situ* hybridizace a denzitometrie prokázaly snížení počtu niterních neuronů a intenzity neuronálního zbarvení na straně poškozeného nervu a současné zvýšení *Ac*NOS mRNA v axoplasmě stejnostranného „nožního nervu" pomocí RT-PCR.

Část dizertační práce se soustředila na identifikaci dalšího funkčně významného hemoproteinu, thyroidperoxidázy z *Aplysie* (*Ac*TPO). Po naklonování *Ac*TPO genu a lokalizaci *Ac*TPO transkriptu v CNS *Aplysie* jsme prokázali i přítomnost několika dalších transkriptů. Tyto transkripty přímo souvisejí s thyroidální signalizační dráhou a naznačují funkci a přítomnost látek podobných thyroidálním hormonům i u plžů.

Téma hemoproteinů v této dizertační práci vedlo dále ke studiu hemové syntetické dráhy, konkrétně šestého enzymu této kaskády, koproporphyrinogenoxidázy (CPO). CPO jsme klonovali z *Aplysie* a dalších organismů *(Chlorophlexus aurantiacus, E.coli)*. Klonované CPO jsme použili při optimalizaci krystalizačních podmínek vedoucích k prvnímu publikování krystalové struktury lidské CPO. Krystalová struktura umožnila udělat další krok k pochopení katalytického mechanismu CPO a na molekulární úrovni objasnit snížení enzymatické aktivity u jednotlivých patologických mutaci hereditární koproporfyrie.

ABSTRACT

Nitric oxide (NO) plays a crucial role in neuronal signaling in a variety of eukaryotic and prokaryotic organisms. Nitric oxide synthases (NOS) are heme-containing monooxygenases that catalyze the oxygen dependent oxidation of L-arginine to NO and L-citrulline. The NO produced by NOS activity is a gaseous molecule that diffuses easily through membranes and acts inter or intracellularly. NO activates metal-containing enzymes, including soluble guanylate-cyclase (sGC) that increase levels of the messenger molecule cyclic 3,5-guanosine monophosphate (cGMP) (1, 2) which in turn mediate various pathophysiological or physiological functions in neurons. Nevertheless, many aspects of nitrergic neurons and NO function in the central nervous system (CNS) are unclear.

The aim of research described in this thesis was to characterize neuronal NOS, proteins metabolically linked to NOS and NO signaling pathways in the CNS of *Aplysia californica (Aplysia)*, a popular experimental model in cellular and system neuroscience. The biochemical characteristics of *Aplysia* NOS *(Ac*NOS*)* described here revealed its calcium-/calmodulin-(Ca/CaM) and NADPH dependence. A representative set of inhibitors for mammalian NOS isoforms also suppressed NOS activity in *Aplysia*. Polyclonal anti-rat nNOS antibodies hybridized with a putative purified *Ac*NOS (160 kDa protein) from partially purified CNS homogenates in Western blot studies. This thesis reports *Ac*NOS activity about six times lower than activity detected in the mammalian cerebellum (3), but was comparable with average values reported for the insect brain (4, 5). Basal levels of cGMP production in *Aplysia* CNS were determined. Stimulation with NO donors and incubation with PDE (phosphodiesterase) inhibitors significantly increased cGMP levels. A specific inhibitor of sGC reduced basal cGMP levels by half and prevented a rise of cGMP in the presence of NO, confirming that NO may indeed function as molluscan CNS messenger, and that cGMP is one of its effectors.

The full length gene of *Ac*NOS was cloned and found to contain all of the conserved sites characteristic of a functional NOS in vertebrates. Nitrergic neurons in *Aplysia* CNS were mapped and localized; around 2% of all central neurons were shown to be nitrergic by means of *in situ* hybridization (ISH) and immunohistochemistry.

A two-color ISH protocol for whole-mount *Aplysia* ganglia was optimized for this thesis work and used to identify neurons and directly correlate functional and protein expression data The complete topographic organization of *Aplysia* mechanosensory neurons expressing neuropeptide sensorin-A was thus assembled.

The effect of unilateral pedal nerve crush on the level of expression of NOS mRNA in *Aplysia* pedal neurons was investigated, to look at the functional implications of NO in nerve regeneration and neuropathic pain. ISH and densitometry showed that the number of neurons and the intensity of neuronal staining following unilateral pedal nerve crush was significantly reduced in cells on the injured side, whereas a concurrent and significant increase of *Ac*NOS mRNA was detected in pedal nerve axoplasm by RT-PCR.

Part of the thesis work concentrated on the identification of another functionally important putative heme-containing enzyme, the *Aplysia* thyroid peroxidase gene (*Ac*TPO). After cloning and localization of *Ac*TPO in the *Aplysia* CNS, several transcripts from the thyroid hormone (TH) signaling pathway were identified suggesting the presence of TH-like signaling in molluscs as well.

The thesis theme of heme enzymes continued with an investigation of the protein necessary for the sixth step of the heme synthesis pathway, coproporphyrinogen oxidase (CPO). CPO was cloned from *Aplysia* and other organisms *(Chlorophlexus aurantiacus, E.coli)*. The cloned CPO genes were used to optimize protein crystallization conditions, leading to the first reported crystal structure of human CPO. The crystal structure enabled some elucidation of the catalytic mechanism of CPO and an understanding at the molecular level of the observed decrease in CPO enzymatic activity in certain pathological mutations of hereditary coproporphyria.

Key words: nitric oxide synthase, cyclic 3,5-guanosine monophosphate, *Aplysia californica*, CNS, heme protein, coproporphyrinogen oxidase, *in situ* hybridization

INTRODUCTION

Nitric oxide (NO) plays a crucial role in neuronal signaling in variety of eukaryotic and prokaryotic organisms. NO produced by nitric oxide synthase (NOS) enzymes is a gaseous molecule that diffuses easily through membranes and acts inter or intracellularly.

Unlike the classical neurotransmitters, NO does not require storage vesicles or exocytosis, and is produced on demand. Tightly regulated NO production is critical for its action ('right amount at the right time a the right place', (6). NO is released in small amounts; it acts locally as a signaling molecule, activating mainly the second messenger cyclic guanosine monophosphate (cGMP)(7), and further various of its effectors. Besides a cGMP activation role, NO has an electron pair that make a radical molecule able to directly act on ion channels (8-10); interact with, or nitrosylate proteins (11, 12) and cyclic nucleotide gated channels (13). The unregulated release of large amounts of NO leads to pathological conditions in sepsis, carcinogenesis and multiple sclerosis. Underproduction of NO also triggers pathological conditions including hypertension, artherosclerosis, septic shock and ischemic reperfusion injury.

In the human central nervous system (CNS), nitrergic (NOS containing) neurons account for roughly 1% of neurons in the cerebral cortex. NO is implicated in neural signaling, neurotoxicity (14), in modulating synaptic plasticity (e.g. long-term potentiation is considered a synaptic correlate of learning and memory, where glutamate binds to N-methyl-D-aspartate (NMDA) receptor and activates NOS (15)), brain development (16), visual processing (17), food and drinking behavior (18), circadian rhytm (19), and in nociceptive neural responses (20). NO plays a role in neurological disorders such as Alzheimer's disease, Parkinson's disease, secondary neuronal cell death after trauma, demyelination disorders (multiple sclerosis). Increased NO levels are also seen in infections like meningitis, affecting the disruption of the blood-brain barrier (21), or in AIDS dementia (22).

Three NOS isoforms have been described in mammals. An iNOS isoform is inducible (inducible NOS type II), and is synthesized in response to elevated cytokine production, inflammatory mediators etc. Two other NOS isoforms are constitutively expressed (neuronal type I, nNOS and endothelial type III, eNOS) and their activity depends on increased calcium levels. The presence of NOS and NOS-like proteins has been documented in different phyla, from bacteria and plants to mammals, but biochemical characterization of NOS in molluscs has been limited. This thesis concentrates on investigating nNOS in the mollusc *Aplysia* that is widely used to model human neurophysiology.

Nitric oxide synthases are hemoproteins that catalyze the production of nitric oxide and L-citrulline by oxidation of L-arginine. NOS functions as a homodimer. Each NOS monomer contains a N-terminal oxygenase domain binding heme, tetrahydrobiopterin and arginine; and a C-terminal reductase domain binding for FAD, FMN, and NADPH. The two domains are linked by a calmodulin (CaM) binding region.

Heme (protoporphyrin IX) with its bound iron, acts as a prosthetic group for a number of proteins ("hemoproteins") with a wide range of biological functions (including nitric oxide synthase, cytochrome P450, catalases, peroxidases, and guanyl cyclase enzymes). Heme biosynthesis, comprised of eight sequential enzymatic reactions, is one of the essential biochemical pathways of life, and occurs in all metabolically active cells. The porphyrin molecules are colored with unique photochemical features (the conjugated double-bond system makes porphyrins resonating compounds, with a typical dark red color and characteristic absorption spectra consisting of a major band near 400 nm, the Soret band, and multiple smaller bands (depending upon the solvent), between 500 and 630 nm).

A partial aim of this study from a biochemical point of view was to approach NOS not only as an enzyme, but also as a heme protein family member. In humans deficiency of individual heme biosynthetic enzymes can lead to the clinical presentation of specific porphyrias. This thesis examines hereditary coporphyria caused by deficiencies of coproporphyrinogen oxidase. Defining the crystal structure of heme biosynthetic enzymes will enable the understanding of catalytic mechanisms of heme synthesis, and very likely of the molecular basis of porphyrias.

The overall aim of the thesis was to characterize neuronal nitric oxide synthase and proteins linked to metabolism and signaling pathway of NOS in the central nervous system of an opistobranch mollusc *Aplysia californica*. *Aplysia* is an effective model organism, widely used in the neuroscience field to study isolated cell interactions as well as for linking together neuronal function and complex behavior. The advantage of *Aplysia* as a model stems from the robustness and ease of identification of its neurons, as well as the relative ease of isolation and detailed characterisation of known neurons and neural networks linked to behavior. Cell culture techniques for isolated molluscan neurons allow researchers to (review see(23)) better define the external variables, and study transmitter – receptor interactions and the action of NO directly on isolated neurons. *Aplysia's* large and identifiable neurons have been used to study the molecular basis of learning and memory(24, 25), cellular correlates of motivational states(26-28), nerve injury and regeneration(29, 30), and motor pattern generation and modulation(31).

Aplysia data on isolated and reconstructed sensory-motor synapses is being extrapolated and linked to results from other species, from invertebrates to humans (23). During the writing of this thesis, genomic information representing 50-70% of the total *Aplysia* transcriptome was sequenced and published (32), giving this project the chance to systematically use a genetic basis for better understanding biochemical characteristics and physiological functions in *Aplysia's* neural system.

AIMS OF THE THESIS

The overall aim of this thesis was to characterize heme protein nitric oxide synthase (NOS) and proteins linked to metabolism and signaling pathway of NOS in the central nervous system of *Aplysia californica* (*Aplysia*), a popular experimental model in neurocellular and neuronsystem science, in order to better understand the role of NO as a physiological neuromodulator and its pathogenesis in a variety of neuronal disturbances and degenerative CNS afflictions. The specific aims of the thesis are listed below.

- to characterize the enzymatic activity of *Ac*NOS and provide biochemical evidence for NO-cGMP signaling in molluscs,(Paper A).
- to clone *Ac*NOS and map NOS-containing (nitrergic) neurons in the *Aplysia* CNS (Paper B).
- to investigate the effect of unilateral pedal nerve crush on expression levels of *Ac*NOS mRNA in *Aplysia* pedal neurons (Paper C), to determine NO contribution to nerve regeneration and neuropathic pain.
- to examine the topographic organization of sensorin-A expressing central neurons in the *Aplysia* mechanosensory system (Paper D), using ISH protocols, and utilizing other techniques (staining by nerve backfill, soma injection and electrophysiological methods) to define the spatial relationship between soma, peripheral axons and receptive fields.
- to optimize a two-color ISH protocol for use on whole-mount *Aplysia* ganglia, in conjunction with intracellular dye labeling to identify and directly correlate functional phenotype with specific gene expression (Paper E)
- to identify another functionally important, putative heme enzyme: *Aplysia* thyroid peroxidase (*Ac*TPO) by cloning and localization, and to assemble evidence of TH-like signaling in mollusks (Paper F).
- to clone the sixth protein from the heme biosynthetic pathway- coproporphyrinogen oxidase from *Aplysia* and to help characterize the crystal structure of its human counterpart (Paper G).

METHODS

Animals. *Aplysia californica* (50-200 g) (Figure 9) were supplied by Marinus (Long Beach, CA), and the NIH-*Aplysia* Resource Facility (Miami, FL). Animals were kept in aquaria containing filtered sea water (FSW) at 15-18°C on a 12:12 light:dark cycle. They were regularly fed on live *Gracilaria* seaweed or dried seaweed laver. Prior to dissection, animals were anesthetized by injecting a volume of isotonic $MgCl_2$ (337 mM) equivalent to 50-60% of their weight.

Preparation of amplified cDNA and cloning. cDNA library preparation was carried out exactly according to (33) (Method A) (Clonetech Kit) or as described in (34) (Ambion Kit) from the whole CNS of *Aplysia*. Cloning of *Ac*NOS was done from the amplified cDNA from the CNS of *Aplysia*. RNA isolation and preparation of amplified cDNA by reverse transcription-PCR was done as previously described(35).

In situ hybridization (ISH) *In situ* hybridization experiments were performed using whole mount preparations of the *Aplysia* CNS. Plasmid containing the full length *Aplysia* genes were subcloned in pGEM-T vector (Promega) in JM-109 E.coli cells. The plasmid was isolated, purified and sequenced to obtain the orientation of the gene. The plasmid was linearized with specific restriction enzymes (*NotI* for the anti-sense probe using T7 polymerase, *ApaI* for the sense probe with Sp6 polymerase) and used as a template for the preparation of specific anti-sense and sense digoxigenin-labeled RNA probes following the Roche protocol for probe preparation with DIG RNA labeling kit (Sp6/T7). Sense probes were used as nonspecific controls and in none of the control preparations using sense probes (twelve preparations) produced any specific staining in the CNS under identical conditions and labeling protocols. Our *in situ* hybridization protocol was based on previously published reports(36, 37) with several modifications.

Dye injection Sensory neurons were impaled with sharp microelectrodes filled with 4% LuciferYellow in 0.1% lithium chloride (LiCl). The same type electrodes had resistances of 5–9Ω when filled with 3M potassium acetate and ~25–40 Ω when filled with 0.1% LiCl. Dye was iontophoretically injected into sensory neurons for 25 min using a continuous train of −2 to −5 nA current pulses with a 600 ms interpulse interval and a 50% duty cycle. After injection ganglia were fixed by flooding the dish with 4% formaldehyde in PBS and left for at least 4 h, but not longer than overnight at 4°C. Following fixation the preparations were rinsed and desheathed as described above.

Measurement of NOS Activity. Following dissection, ganglia were homogenized in approximately 5 vol. of buffer containing 25mM Tris-HCl (pH 7.4), 1mM EDTA, 10 mM EGTA with a tissue homogenizer on ice. The homogenate was centrifuged at 14,000x g for 5 min. at 4°C and the pellet was discarded. NOS activity was determined according to the method described previously (3).

cGMP assay. Following dissection *Aplysia* central ganglia were incubated for 1 h with IBMX (3-isobutyl-1-methylxanthine, non-specific PDE inhibitor (38) dissolved in DMSO (dimethyl sulfoxide, 1mM, from Fischer) at RT, and/or with 1H-[1,2,4] oxadiazolo [4,3-a]

quinoxaline-1-one (ODQ, 1mM) (39). The control group was incubated with 1% DMSO. Then the CNS was incubated for 10 min with NO donors SNAP (*S*-nitroso-*N*-acetylpenicillamine, dissolved in DMSO, 1mM) or with DEA/NONOate (Diethylammonium (Z)-1-(N,N-diethylamino)diazen-1-ium-1,2-diolate, 1mM) (40). After incubation ganglia were transferred into a boiling acetate buffer (400 µl at pH 5.8, 0.5 M), and incubated for 3 min.at 100°C, then mechanically homogenized and spun at 13000xg for 10 min at 4°C ((41). The homogenate was diluted 10x in the acetate buffer and the cGMP levels were assessed using the RIA cGMP[^{125}I] assay from Amersham Biosciences following the manufacturer's protocol.

Western Blot. *SDS-PAGE* was performed as first described by Laemmli (42). 1-3 µg of the denatured protein was applied per lane to an SDS gel (10%T, 2.6%C) and separated in a Bio Rad mini-gel apparatus at 20 mA for about one hour or until the dye front approached the bottom of the gel. Gels were removed and either stained in coomassie blue or transferred to a PVDF membrane. Coomassie staining was performed for about 30 minutes at room temperature in a solution of 2% CB G250, 7.5% HAc, and 50% MeOH. Destaining was carried out in 7.5% HAc, 15% MeOH. Electrotransfer (43) to a 0.2 µ PVDF membrane was performed in a Bio Rad Mini Trans-Blot apparatus following manufacturer's instructions. The transfer buffer was 24 mM TRIS, 19.5mM Glycine, pH9.2, and the running conditions were 100 volts for one hour. Detection was performed with a polyclonal antibody raised against rat neuronal NOS (rabbit) and visualized with alkaline phosphatase color reagent. Briefly, the membrane was blocked with 1% non-fat dry milk, 1% BSA, in TBS (20 mM TRIS/HCl, pH 7.4, 0.5 M NaCl) for one hour. The membrane was then incubated for one hour with a 1: 2-3000 dilution of antibody in TTBS (asTBS, plus 0.05% Tween 20). After extensive washing in TTBS, goat anti-mouse IgG alkaline phosphatase conjugate (ZYMED, 81-6522) was used as a secondary antibody, again for one hour. Visualization was accomplished by gentle rocking in NBT/BCIP reagent.

Nerve crush. After injecting isotonic $MgCl_2$ solution (equivalent to about 30% of body weight) with the animal suspended in a chamber containing FSW a small incision was made in the skin to expose the pedal ganglia. Peripheral left or right pedal nerves were crushed using fine forceps at a distance of approximately 1 cm from the pedal ganglion The incision was sutured immediately after all the ipsilateral peripheral nerves from the pedal ganglion had been crushed (modified from(44)).

RT-PCR. cDNA made from each sample was used to amplify specific fragments by PCR (40 cycles), using specific primer sets for the following: (1) neuronal nitric oxide synthase (NOS) (GenBank accession numberAAK83069), nt 3610-4049; (2) SN-specific neuropeptide sensorin A (GenBank accession number X56770), nt 43-331; (3) beta-thymosin (GenBank

accession number AF454398, nt 61-195. All the reactions were assembled, amplified, and analyzed at the same time.

Iodine Incorporation and TH synthesis. We exposed larvae at the developmental stage when adult spicules had formed for 8 hours in 12 well plates to experimental treatments. We placed 50 randomly chosen larvae into each well, containing 4ml of solution (10^{-3}M thiourea and the buffer-only control respectively). All solutions were made up in SW^{125} (MPFSW with I^{125} at 51937 dpm; Carrier free specific activity of I^{125} was 642.8GBq/mg). Aplysia juveniles were processed in a similar way except that we used 10^{-2}M thiourea in the inhibitor treatment.

To test whether I^{125} that the larvae had incorporated was built into T4, we prepared samples for thin layer chromatography (TLC). We added 1ml of ice cold MeOH to each sample after the sample was counted [samples containing I^{125} were counted on a ssMPD instrument (BioTraces, Inc., Herndon, VA) in standard mode. After vortexing all samples we centrifuged them at 1980g for 10 minutes and collected the supernatant. Then we spiked the samples with 100µl non-radioactive 10^{-4}M T4 (thyroxine; Sigma-Aldrich T-1774) and T3 (3,3",5-Triiodo- L -thyronine; Sigma: T2877) and then concentrated in a speed-vac to complete dryness. The dry pellet was redissolved in 30µl 0.01N NaOH. All 30ul were loaded on a TLC plate (Whatman LK5D silica gel 150A with fluorescence marker; Whatman #4851-840) and run for 1.5 hours in a 2-methylbutanol/*t*-butyl alcoholy/25%NH3/acetone, 7:14:14:56, v/v solvent. We visualized the cold T4 and T3 markers under UV light on a BioRad™ Fluor-S Multilmager system and radioactive bands on a Molecular Dynamics™ Phosphorimager SI. Overlaying the UV image with the one from the phosphor imager allowed us to compare the radioactive bands to our TH standards.

TH measurements in sea urchin larvae and Aplysia haemolymph. We collected *Aplysia* haemolymph samples. 5 volumes of 100% ice-cold MeOH was added to samples. Extraction was done at 4°C overnight. We then centrifuged samples at 3000rpm for 10 minutes at 4°C. We decanted the liquid upper phase and kept the pellet for protein analysis. The upper phase was brought to complete dryness in a Speed-Vac and then resuspended in 50ul 0.01N NaOH. The pellet was redissolved in 100µl 1N HCl at 60°C for one hour and then vortexed at full strength for 1 minute per sample.

For TH analysis we used the ELISA KIT (Total Thyroxine (Total T4) ELISA Kit Alpha Diagnostic International, Inc.; TX, USA) following the manufacturer's instructions. For Protein analysis we used Pierce micro BCA kit as per manufacturer's instructions.

Phylogenetic analysis.. The alignment was done using ClustalX (EBI European Bioinformatics Institute (Oxford, United Kingdom) (45) with default parameters, all gaps were removed manually in GeneDoc prior to tree construction. Sequence analysis and

phylogenetic tree building was done in the program TREEPUZZLE (http://www.tree-puzzle.de) with the default parameters and 10,000 iterations of the maximum likelihood algorithm. The tree itself was drawn with Treeview. The conserved domains were confirmed using Swissprot and Prosite databases (for further details see methods in attached paper E).

Data Analysis. Data were organized and analyzed in Excel and SPSS. Statistical comparisons between the experimental treatments and the controls were done using Student's t-test, ANOVA with simple contrast or MANOVA. For all analyses we used SPSS. Results are presented as: mean difference (treatment value minus control value) ± one S.E.; p-value. If the mean difference is positive this means that the value in the experimental treatment was larger than the value in the control. All p-values are from null hypotheses testing that the mean difference mentioned above equals 0. Information on Aplysia ESTs was derived from the *Aplysia* neuronal transcriptome(32).

Protein Preparation and Crystallization. Human CPO homodimer (monomer Mr 39,248) was expressed and purified as described (46). To overcome the time-dependent proteolytic cleavage, we devised a cross-seeding strategy. First, we obtained crystals of a bacterial CPO (*Chloroflexus aurantiacus*, a thermophilic phototroph). These were grown in sitting drop vapor diffusion setups at 22 °C from a reservoir buffer containing 30% MPD and 100 mM cacodylate buffer, pH 6.5. Crystals obtained under these conditions belong to the hexagonal space group (P6122) with cell dimensions 205.53 x 205.53 x 85.92 Å, α= 90°, ß= 90°, γ= 120°, and easily diffract X-rays to a Bragg spacing of 1.9 Å. Second, seed stocks of *C. aurantiacus* CPO crystals were prepared and used to streak seed into pre-equilibrated solutions containing fresh human CPO (40 mg mL-1), 20% MPD, 0.05 M Tris-HCl pH 7.5, and 10 mM sodium citrate as an additive. Cubic shaped crystals appeared after 48 hours. Mature crystals were stabilized in a glycerol-containing cryoprotectant prior to flash freezing in liquid nitrogen.

Structural Determination. Data from a native crystal were collected to a Bragg spacing of 1.5 Å using an ADSC Quantum-315 detector at beam line 9-2 of the Stanford Synchrotron Radiation Laboratory. Multiwavelength data on Se-Met human CPO crystals were collected on an ADSC Quantum-4 CCD detector at beamline 5.0.2 of the Advanced Light Source, Berkeley. All data sets were integrated and scaled using the HKL2000 package and the statistics are reported in Table I (which is published as supporting information on the PNAS web site). Equilibrium Analytical Ultracentrifugation. 120 µL of wild-type human CPO was sedimented to equilibrium at two different loading concentrations (A280 of 0.32 and 0.4), five different speeds (18.0, 22.1, 23.4, 26.2, and 28.0 krpm) and, at 4 °C in a double-sector, epon-filled centerpieces using an AN60 TI rotor in a Beckman Optima XL-A analytical ultracentrifuge. Scans were taken at 280 nm once equilibrium was established by scanning

with 20 averages at a 0.001 cm radial step size setting. Data were globally fitted using the NONLIN software package.

CHAPTER I.

CLONING, LOCALIZATION AND CHARACTERIZATION OF NITRIC OXIDE SYNTHASE IN *APLYSIA CALIFORNICA*

RESULTS AND DISCUSSION I.

A. Characterization of *Aplysia*NOS [#]

Our goal was to characterize NOS from *Aplysia.* We examined the effect of calcium chelators and cofactors on NOS from the CNS of *Aplysia* and tested well known mammalian, isoform-specific NOS inhibitors on *AcNOS*. The connection to functional importance was tested by assessing the NO induced cyclic guanosine monophosphate (cGMP) upregulation, with or without the presence of phosphodiesterase inhibitors. Some pharmacological evidence, together with an effect on evoked excitatory postsynaptic potential (EPSPs) for signaling mediated by NO via cGMP in the metacerebral cells (MCC, a pair of serotonergic modulatory neurons in the cerebral ganglia) of *Aplysia* has been already provided by Koh, 1998 (47).

NOS present in the CNS of Aplysia is calcium dependent

The relative NOS activity and the role of cofactors in the CNS of *Aplysia* is shown in Figure I. as an L-[14C]arginine/L-[14C]citrulline conversion. The production rate of L-[14C] citrulline from homogenized ganglia was 22.2 ± 4.0 pmol/mg of protein/min. Importantly, Figure 10 illustrates that *Ac*NOS activity was shown to be Ca-dependent; the documented values for Ca-free conditions in the media containing EGTA were below 40% of the control NOS. Exclusion of NADPH from the reaction caused a reduction in *Ac*NOS activity to less than 35%. Addition of W-7 hydrochloride, a Ca/CaM-dependent phosphodiesterase (PDE) inhibitor, also significantly reduced L-[14C]citrulline production to less than 60.

The effects of vertebrate isoform specific NOS inhibitors on *Aplysia* NOS were studied and the most potent inhibitor proved to be L-thiocitrulline (an inhibitor of mammalian nNOS and iNOS) which reduced theNOS activity by 95% ($P < 0.005$). All other tested NOS inhibitors caused a significant reduction in L-[14C]citrulline production: S-Ethyl-ITU hydrobromide (a selective inhibitor of all vertebrate NOS isoforms) by 85% ($P < 0.050$) and L-NIL

dihydrochloride (iNOS inhibitor) by 78% ($P < 0.05$). The competitive NOS inhibitor L-NAME suppressed the NOS activity by almost 60%..

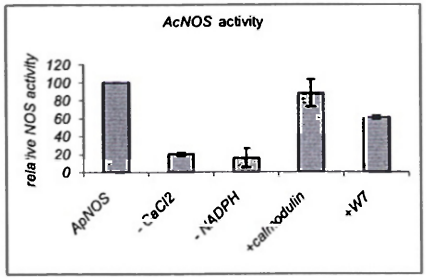

Figure 1. Co-factor dependence of *AcNOS*. Relative NOS activity is shown as a percentage of *AcNOS* activity (L-[14C]arginine/L-[14C]citrulline conversion in homogenates of the CNS of *Aplysia*). Contr, control conditions with all co-factors; -CaCl2, without CaCl2; -NADPH, without NADPH; in the presence of calmodulin (+CaM); +W7, in the presence of 5 mM W 7 hydrochloride (a potent Ca/CaMdependent phosphodiesterase inhibitor). Student's t-test was used for statistical analysis of the observed differences. Data are the mean of three experiments ±SEM values. See additional details in the text.

PDE inhibitors and NO donors both increase cGMP in the CNS of Aplysia

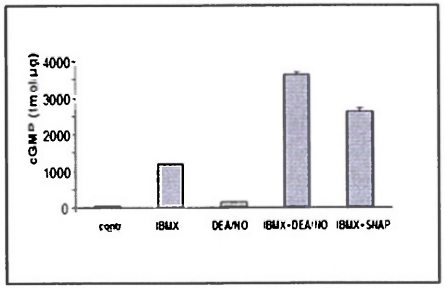

Figure 2. Pharmacology of *AcNOS*. Relative NOS activity is shown as a percentage of L-[14C]arginine/L-[14C]citrulline conversion in the presence of several inhibitors of mammalian NOSs. Contr, control conditions with all co-factors; + L-NAME, in the presence of 500 IM L-NAME (a competitive NOS inhibitor); + D-NAME, in the presence of 500 IM D-NAME (less active enantiomer of L-NAME), + L-NIL, in the presence of 5 mM L-NIL dihydrochloride (iNOS inhibitor); +thiourea,

in the presence of 5 mM S-Ethyl-ITU hydrobromide (selective inhibitor of all vertebrate NOS isoforms); and with 5 mM Lthiocitrulline (an inhibitor of nNOS and iNOS).

The cGMP levels from the RIA cGMP[125I] assay are shown as converted per 1 lg of total homogenized protein (Figure 2). The basal level of cGMP in the CNS was 44.47 fmol/µg. Incubation with the NO donor DEA/NONOate (1 mM) increased the cGMP activity almost 3.5 times, whereas incubation with non specific PDE inhibitors increased the cGMP levels 26 times. Following 1 h incubation with IBMX (1 mM) the increase of cGMP was 58–61 times higher compared with the basal level of cGMP. Further, selective inhibition of soluble guanylyl cyclase with ODQ (1 mM) incubated simultaneously with the NO donor DEA/NO (1 mM) even reduced the cGMP activity compared with basal cGMP levels. The co-incubation of ODQ. DEA/NO and IBMX still kept the cGMP activity 2.4 times below normal.

Western blot and immunohistochemistry

(Figure 3). Partially purified *Ac*NOS run on SDS-PAGE gel, then reblotted and hybridized with a preadsorbed polyclonal rabbit anti-rat nNOS antibody showed a clear band around 160 kDa. A similar immunopositive band at 150 kDa was detected in our control rat cerebellum homogenate.

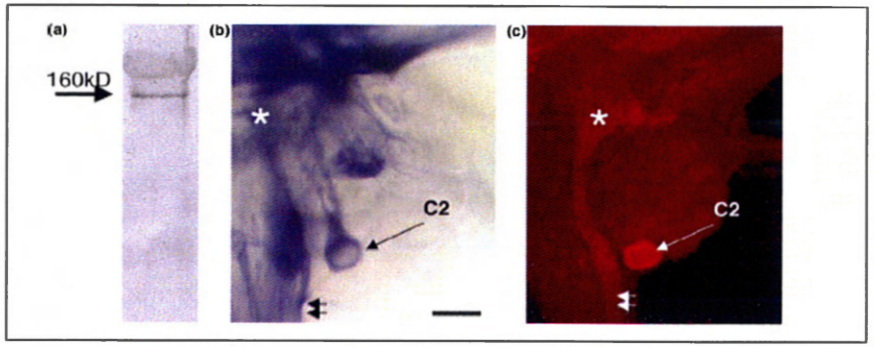

Figure 3. Western blot and immunostaining in the CNS of *Aplysia*. (a) Partially purified *Ac*NOS is from the CNS cross reacted with a preadsorbed polyclonal antibody to rat neuronal NOS and is recognized as a protein with molecular mass of cca 160 kDa (a). (b) NADPH-diaphorase histochemistry in the lateral part of the cerebral ganglion (E-cluster area); (c) NOS immunoreactivity with rat polyclonal NOS antibodies reveals similar patterns of labeling in the same region of the cerebral ganglion. Large arrows in (b and c) indicate the position of the identified neuron (C2) also know to be nitrergic and located in this area of the cerebral ganglion. Small arrows mark specific labeling in nerves and (*) point out the staining in ganglionic neuropil.

In this study we documented that functionally active NOS is present in the CNS of *Aplysia californica* and for the first time it is shown to be calcium dependent. *Aplysia* NOS shares common enzymatic characteristics with constitutive mammalian and insect neuronal NOS as a calmodulin and NADPH dependent enzyme. Thus, the observed Ca-dependence of *Aplysia* NOS confirms an earlier hypothesis that the rise of intracellular Ca2+ (either following activation of transmembrane Ca-channels or from intracellular stores) might act as a physiological regulator of NO synthesis in the molluscan CNS. In this repect, *Ac*NOS was similar to the NOS described in two representatives of pulmonate molluscs, *Lymnaea stagnalis* (48) and *Helix pomatia* The pharmacological profile of *Aplysia* NOS was similar but not identical to NOS described for other species. The *AcNOS* showed closest similarity to mammalian neuronal NOS, although selective inhibitors of two other mammalian isoforms (eNOS and iNOS) had a significant suppressive effect as well. There is relatively little known about the structure of NOS-related proteins in molluscs. For example, partially purified NOS protein from *Aplysia* CNS displayed a band with molecular mass of approximately 160 kDa and a very faint band around 175 kDa. The shorter band is comparable in size with the 150 kDa of denatured rat nNOS protein (49). The molecular mass of insect NOS protein was around 130–155 kDa (4, 5) but, surprisingly, the immunoreactive NOS protein in the mollusc *Helix pomatia* with the highest reported enzymatic activity showed only a band of 60 kDa (50). The fact that NO induces cGMP synthesis and immunoreactivity through activating soluble guanylyl cyclase has already been shown (7, 51, 52) for many species including some molluscs (47, 53, 54). However, direct biochemical measurement of soluble guanylyl activity in molluscs has been performed only on a representative of land pulmonates, *Helix pomatia* (41). Here, we determined the basal levels of cGMP production in the CNS of *Aplysia* and showed that it significantly increased following stimulation with NO donors (>3-fold), and incubation with PDE inhibitors (>20-fold). Importantly, a specific inhibitor of soluble guanylyl cyclase (ODQ) reduced by half the basal level of cGMP in the CNS of *Aplysia* and prevented the rise of cGMP by NO. These results suggest the substantial tonic production of NO in the intact CNS and its link to cGMP pathways. In summary, we directly showed that enzymatically active Ca-dependent NOS is present in the CNS of *Aplysia* and that it can act via cGMP signaling. Biochemical and pharmacological characterization of these two signaling pathways provide a foundation to further examine their interactions and functional role in neuronal networks using *Aplysia* as a model organism.

In this work my contribution was to biochemically characterize the *AcNOS* by measurement of NOS activity, cGMP assay, Western Blot, and immunohistochemistry.

B. Cloning of *Aplysia* NOS and its localization in the CNS [#]

Cloning of Aplysia nitric oxide synthase (AcNOS)

The cDNA of 4444-bp has been cloned, with an ORF of 4161 bp and conceptual translation yielded a protein of 1387 amino acid residues (*Ac*NOS; GeneBank accession number AF288780). The sequences contain all putative conserved cofactor and substrate binding sites. Three molluscan full length cDNA sequences of NOS proteins, from *Lymnaea stagnalis* (Korneev 1998) and *Aplysia* (Sadreyev, 2000), and last year a NOS from terrestrial slug *Lehmannia valentiana* (Matsuo, 2007) have been published. The analysis of highest BLAST homology (55) of these molluscan NOS sequences reveals the maximum identity of 73% with *Lehmannia* and 61% with *Lymnea*. From the three vertebrate NOS isoforms, the molluscan sequences share the highest homology with human neuronal NOS (54% with *Aplysia*), suggesting a similar function.

In situ hybridization in the CNS of Aplysia californica

To describe a topographic distribution of *Aplysia* nitrergic neurons in the CNS we used the full length clone of *Ac*NOS (see section above) for the in situ hybridization (Figure 4). The staining was specific, with darkly labeled NOS containing neurons. Control animals (labeled with sense mRNA) showed no staining.

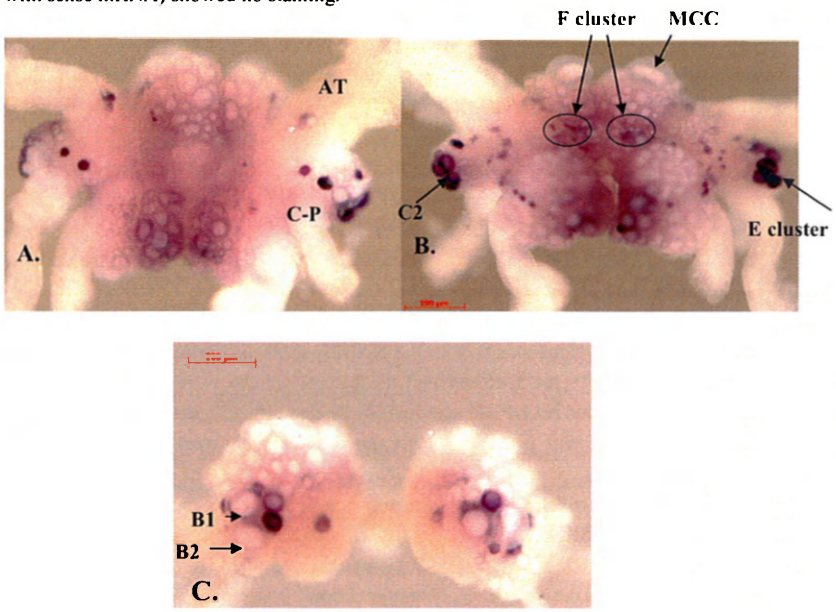

Figure 4. *In situ* hybridization with antisense full/length RNA probes with DIG-labelled NTPs to *Ac*NOS mRNA produced intense and specific labeling throughout the CNS. (A) Ventral view of the cerebral ganglia (B) Dorsal view of the cerebral ganglia. (C) Caudal view of the buccal ganglion. Anterior tentacular nerve (AT), the cerebro-pedal (C-P) nerve, metacerebral cell (MCC), B1,B2,C2-neurons.

ganglion	number of nitrergic cells (n=4-10)	cell size
CG	2x(13-30) in F cluster 2x(7-15) in E cluster 2x(7-10) in B cluster 2x(25-38) isolated n.	(9-186)
BG	2x31-53	(15-129)
AG	17-26	
PeG	2x(12-29)	(15-101)
PlG	2x(1-4)	(10-33)

Table 1. Counts and soma size of nitrergic neurons in the *Aplysia* ganglia

To study the role of NO on the level of individual neurons we cloned the nitric oxide synthase from a model organism *Aplysia* and mapped NOS-containing (nitrergic) neurons in the CNS using *in situ* hybridization and immunocytochemistry. A similar pattern of NOS expression was observed with both techniques and matched the known distribution of NADPH-d reactive neurons in the CNS. Up to 390 central neuronal somata were found to be labeled with NOS selective RNA-probes including several identified neurons, which corresponds to 1-2% of nitrergic neurons described in mammals (Table 1). The majority of nitrergic neurons were located in the cerebral (~145) and buccal (~84) ganglia followed by pedal (~41), abdominal (~21) ganglion and pleural (~8) ganglia. NOS containing cells were detected at the periphery in chemosensory areas such as the mouth area, rhinophores, tentacles. The intensity of the staining between distinct populations of neurons varied considerably even within one ganglion, but the pattern of intensity of staining together with the localization of stained somata was preserved between individuals. A gradual scale of intensity of staining corresponds with the NADPH-d labeling published earlier, where the NOS-positive cells in the E-cluster and the pleural ganglia were the darkest (56). NOS specific antibodies and NADPH-d activity (56) labeled primarily neuronal processes and the ganglionic neuropil; with neuronal somata showing relatively weak staining intensity. This finding suggests that the major NOS activity is associated with neurites. Furthermore, *in situ* hybridization also confirms the presence and transport of NOS-specific mRNAs to distant processes (unpublished observation, Buganova and Moroz). In addition, NOS containing cells were detected in the neuropil and at the periphery. Patterns of NOS distribution implies an important role for this enzyme in diverse networks including feeding and locomotion.

The cloned *Aplysia* NOS gene sequence contains all of the conserved sites characteristic of a functional NOS; these sites are implicated in interactions with L-arginine, heme, tetrahydrobiopterin, calmodulin (CaM), FAD, FMN, and NADPH, in Zn2+ binding and in dimerization.

My contribution was to cooperate on cloning the full length *AcNOS* gene, and utilize it for *ISH* to localize and map the *AcNOS* mRNA in the *Aplysia* brain

C. Nerve injury in *Aplysia* reduces nitric oxide synthase mRNA levels in neuronal somata while increasing mRNA levels in axoplasm.

Nitric oxide (NO) signaling in mammals is thought to contribute to nerve regeneration and neuropathic pain. *Aplysia* sensory and motor neurons with axons in pedal nerves have proven useful for investigating similar responses to nerve injury, including sensory hyperexcitability involving the NO-cGMP pathway. Here we describe alterations in nNOS mRNA expression in pedal ganglion neurons and injured pedal nerves following nerve crush.

ISH of control pedal ganglia showed that neuronal somata expressing nNOS mRNA form a discrete cluster of 25-50 cells situated between the pedal-pleural and pedal-pedal connectives and pleural ganglia. After unilateral pedal nerve crush, the number of pedal neuron somata expressing nNOS mRNA was significantly decreased 3 or more days after ipsilateral pedal nerve crush (14.6± 1.6 cells per pedal ganglion, tested at 3, 5, 6, 10, and 21 days) compared to contralateral control ganglia (34.3 ± 2.1 cells) or to ipsilateral ganglia tested 1 day after crush (30.7 ± 0.7 cells). In addition, densitometry analysis showed that the intensity of staining was reduced in cells on the injured side. In contrast, a significant increase of nNOS mRNA was detected from pedal nerve axoplasm by RT-PCR 3 days after nerve crush, and preliminary evidence using in situ hybridization suggests that this mRNA accumulates at the crush site. A tentative hypothesis to explain this altered pattern of expression is that nNOS mRNA in the soma decreases because of its translocation to the injury site for peripheral translation during adaptive responses to nerve injury.

D. Protocol for double chromophorelabeled *in situ* hybridization

The non radioactive *in situ* hybridization allows for simultaneous detection of two different transcripts in the same molluscan brain using different colours, with the opportunity to use the protocol to identify colocalization of neurotransmitters, or other substances. The excellent preservation of morphology in whole mount preparations together with the high sensitivity for mRNA detection warrant the use of the protocol in systemic studies of expression patterns of different mRNA, and following electrophysiology experiments with

intracellular dye labeling, making it possible to couple localization of transcripts with electrophysiological studies in positively identified neurons (57).

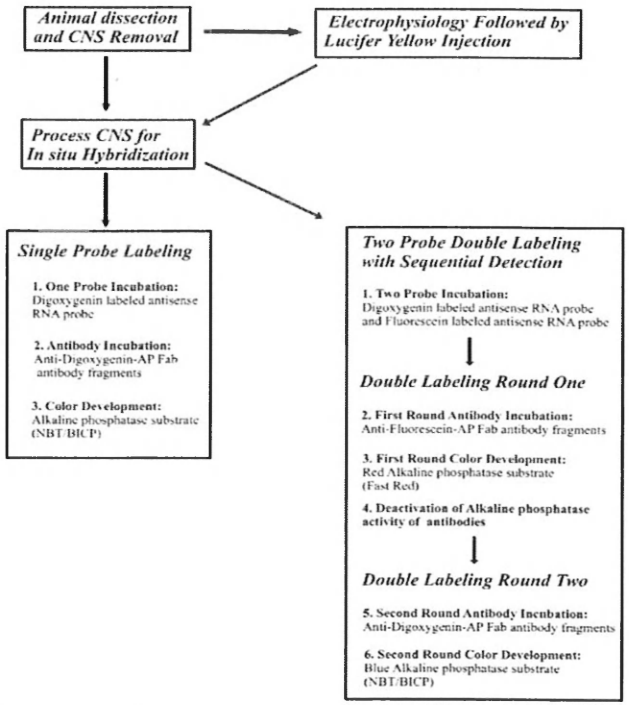

Figure 5. An overview of the *in situ* hybridization protocol. The left side outlines the basic steps of the in situ hybridization. Optional variations are shown on the right. Lucifer Yellow may be injected prior to fixation of ganglia to specifically mark neurons after electrop hysiological tests. For two-color *in situ* labeling, two probes are hybridized at the same time and detected separately by sequential antibody incubations and color development reactions on separate days. Each probe and antibody incubation is done overnight, thus the procedure takes at least 3 days to complete for single labeling and 4 days for double labeling.

Several *in situ* hybridization protocols have previously been applied to the CNS of *Aplysia* (58-60) but most were adapted to sectioned tissues or cultured neurons (61). Ono and McCaman (1992) described an alkaline phosphatase-based *in situ* hybridization method for whole mount *Aplysia* ganglia; however, the protocol was not able to consistently detect expression of the abundant transcript for the neuropeptide FMRFamide (Figure 6B) in

identified cells such as R2 where it is known to be expressed. The described protocol (Figure 5, for detail see thesis) differs from previous *Aplysia* protocols in that it is optimized for processing whole ganglia, produces consistent staining for neuropeptides, and is sensitive enough to detect less abundant transcripts. Expression patterns of two highly abundant neuropeptide transcripts, sensorin (62) and FMRFamide (63), and one relatively low abundant transcript, fasciclin (64) (Figure 6A) are shown as illustrative examples. Some parts of this protocol have been published previously (65-67).

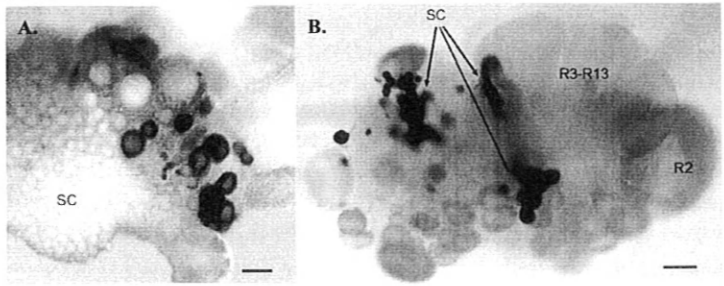

Figure 6. (A) Chromogenic *in situ* hybridization allowed detection of low abundance transcript-fasciclin expression in the right caudal buccal ganglion imaged in a 100% ethanol bath..
(B) Double labeling for sensorin (dark blue precipitate- the substrate of AP is NBT/BICP) and FMRFamide (red- substrate for AP is FAST Red) indicates the respective positions of sensory clusters and cells expressing FMRFamide. Dorsal view of the abdominal ganglion. The giant cell R2, which is the contra-lateral homolog of LPl I is intensely stained while the cluster containing cells R3–R13 is not. The ganglia in were imaged in a glycerol bath. SC, sensory clusters. Scale bars = 100μm.

My contribution to this study was to introduce the double-chromophore labeling in *Aplysia*, and together with Dr. Sami Jezzini to optimalize the *in situ* hybridization protocol for whole mount preparations and as well as following electrophysiology experiments.

E. Somatotopic Organization and Functional Properties of Mechanosensory Neurons Expressing Sensorin-A mRNA in *Aplysia californica* "

Sensorin- A, a neuropeptide, was identified in the pleural VC cluster of *Aplysia*, by Brunet and colleagues (1991). Physiological experiments demonstrated that sensorin-A, could act as an inhibitory cotransmitter at VC cell synapses and imaging experiments showed that sensorin-A is selectively expressed in all of the known mechanosensory clusters in the central ganglia of *Aplysia* and appeared to be absent from all other cells of the CNS (62).

Number and distribution of sensorin-A-expressing neurons

In adult *Aplysia*, all of the somata labeled by sensorin-A antisense probes in our whole mount preparations were in central ganglia; none were in peripheral ganglia or other tissues. The labeled somata correspond to previously described mechanosensory clusters (62) in the abdominal, pleural, cerebral, and buccal ganglia.

Approximately 1000 cells express sensorin-A mRNA in young adult animals (10-30 g) and 1200 cells in larger adults (100-300 g). Thus, sensorin-A-expressing neurons represent 5-10% of all neurons in the CNS (68 2001). All of the labeled somata are in the CNS, primarily in the abdominal left E cluster (LE) , right E (RE), right F (RF), and rostral LE (rLE) clusters (69, 70), pleural ventrocaudal (VC) clusters (71), and the J and K clusters in the cerebral ganglia (72), and buccal S clusters (73) (for detailed pictures see the attached original publication). Expression also occurs in some sparsely distributed cells in most ganglia.

Somatotopic organization of sensorin-A expressing neurons

The results complete the macroscopic map of the peripheral receptive fields of sensorin-A-expressing cell clusters. Our study confirms earlier descriptions of receptive fields in *Aplysia* (69-73) and provides new information about coverage of the midbody and anterior body by the pleural VC clusters, of the rhinophores and propodium by the cerebral J clusters, and of the lip region and buccal mass by the buccal S clusters. When all of this information is combined, sensorin-A-expressing cells are seen to provide a centrally distributed map of the entire surface of the body (see Figs in the attached original paper).

A clear (albeit rough) topographic relationship was demonstrated between the location of each sensory neuron soma in the VC cluster (Figure 7) and both the location of its peripheral receptive field and the nerve carrying its primary axon. Thus, each VC cluster forms a somatotopic map of most of the ipsilateral body surface- an "aplunculus" (Figure 7).

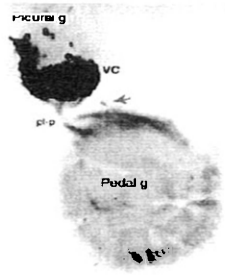

Figure 7. Somatotopic representation of mechanosensory receptive fields in the VC cluster.

Somata in pleural, and pedal ganglia labeled by in situ hybridization with antisense probe to sensorin-A Mrna

Relatively deep focus on a whole-mount preparation of the right pleural and pedal ganglia from a 30 g animal after clearing and embedding. This revealed labeled cells throughout the VC cluster and a smaller, more lightly labeled cell in the pedal ganglion (arrow). Note the intense labeling of neurites in the pleural-pedal connective (pl-p) and the neuropil throughout the pedal ganglion

My contribution to this study was to perform the in situ hybridization and densitometry, with evaluation of the results, together with the mapping of sensorin-A expressing neurons.

F. Cloning of an *Aplysia* hemoprotein,Thyroid Peroxidase, and Characterization of Thyroid Hormone-like signaling in *Aplysia*

The aim was to identify other functional, putative heme enzymes. The putative thyroid peroxidase gene sequence from *Aplysia* (*Aca*TPO) showed high sequence similarity with peroxidasin and thyroid peroxidases, which are the critical thyroid hormone (TH) synthesis enzymes found in all vertebrates. Spatial and temporal expression patterns of these transcripts suggest a role for *Aca*TPO in a variety of processes such as developmental metamorphosis and regulation of the animal's energy metabolism.

Iodine incorporation and TH synthesis in Aplysia is inhibited by thiourea

We exposed juvenile *Aplysia* to I^{125} in order to test whether 1) iodine is incorporated and 2) incorporated iodine is used for TH synthesis (thyroxine and triiodotyrosine). Our results from the thin layer chromatograms confirm that *Aplysia* juveniles used incorporated 1125 to make THs (Figure 8B). Interestingly, *Aplysia* juveniles primarily synthesize T3. Thiourea inhibited TH synthesis in *Aplysia* (Figure 8B). Finally, we were able to detect T4 and T3 in haemolymph of adult *Aplysia* (Figure 8A.) using ELISA. Note that all measurements are standardized to the protein content of the samples.

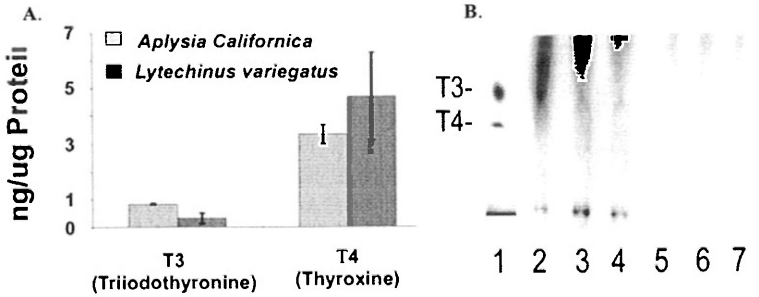

Figure 8. *Lytechinus variegatus* larvae and *Aplysia californica* juveniles incorporate 1125 and build THs with it. Both species contain measurable TH levels. A) We measured T4 and T3 in sea urchin larvae and *Aplysia* juveniles using ELISA and found both hormones present in both species at different concentration. Note that all measurements are standardized to the protein content of the samples. T4 was present at higher concentrations in both species. DPM: decays per minute, B). Incorporated iodine is used to synthesize T3 in *Aplysia* and neither T4 nor T3 was detected when juveniles were exposed to thiourea before extraction. (B; control: lane 2-4, standard: lane 1, +thiourea (10-2):lane 5-7

Cloning of TPO from molluscs

As a first step to elucidate the mechanisms of TH-like synthesis in non-chordate animals we cloned two partial sequences of peroxidases closely related to peroxidasin and thyroid peroxidase from *Aplysia* (*Aca*TPO). *Aca*TPO clusters together with peroxidasin from *Drosophila melanogaster* (DmPsdn) and Humans (HsPsdn) (cluster C). Note, that neither LvTPO nor *Aca*TPO clusters together with human or rat thyroid peroxidase (cluster B). Cluster A consists of other peroxidases with various functions.

*Aca*TPO is 576 amino acids long and has also all major domains necessary for peroxidase function conserved. These are proximal and distal histidine in positions 25 and 273, Ca2+ binding domain in positions 104 (T), 106 (F), 108 (D) and 110 (S). Finally arginine is found in position 77 and asparagines in position 357. While Human (HsTPO) and *Ciona* thyroid peroxidases have complement control protein (CCP) modules (also known as short consensus repeats SCRs or SUSHI repeats) towards the 3 prime end of the gene, *Aca*TPO does not have such a motive. A second calcium-binding EGF-like domain present in CiTPO and HsTPO are lacking in these genes. In addition, AcaTPO is significantly shorter than CiTPO and HsTPO. Thus, *Aca*TPO can be characterized as peroxidase based on its conserved residues. Based on their sequence similarities and topology of the phylogenetic tree we suggest that *Aca*TPO can be classified as possible thyroid peroxidase orthologue.

Our results revealed the presence of thyroid peroxidase transcripts in the *Aplysia* F-cluster, a putative neuro-endocrine center located in the cerebral ganglion. The in frame translation of *Aca*TPO yielded a protein of 576 AA. TPO belongs to the animal peroxidase superfamily and catalyzes three reactions critical for thyroid hormone (TH) synthesis. The presence of this gene in the CNS of *Aplysia* along with several other transcripts from the TH signaling pathway (thyroid-stimulating hormone beta subunit, thyrotropin receptor, thyroxine deiodinase, thyroid hormone binding protein and others) suggest the presence of TH-like signaling in molluscs as well. In this study we provide further evidence of the presence of this signaling pathway by showing that *Aplysia* synthesizes both T4 (thyroxine) and T3 (triiodotyrosine) endogenously using ELISA. We then confirmed uptake of radioactive iodine by juvenile *Aplysia* and showed that this iodine is incorporated into T3. Finally we were able to clone newly identified regulatory genes upstream of thyroid hormone synthesis indicating that a large part of the TH signaling machinery might be present in the sea hare, *Aplysia*.

These studies # were performed in cooperation with Prof.Moroz's lab at the Whitney Laboratory, Saint Augustine, FL, USA. My contribution to this study was to identify and clone peroxidasin and thyroid peroxidase from *Aplysia* (*AcaTPO*)., to localize the TH in *AcNOS* CNS using *in situ* hybridization, and to perform the phylogenetic analysis.

CONCLUSIONS FOR CHAPTER I.

A. Publication A provided evidence that functionally active NOS is present in the CNS of the mollusc *Aplysia californica* and for the first time it was shown to be calcium dependent. *Ac*NOS activity was around six times lower than that in the mammalian cerebellum (3), but was comparable with the average values reported for the insect brain (4, 5). The basal levels of cGMP production in the CNS of *Aplysia* were determined and found to be significantly increased following stimulation with NO donors and incubation with PDE inhibitors. Importantly, a specific inhibitor of sGC (ODQ) reduced the basal level of cGMP in *Aplysia* CNS by half and prevented the NO-induced rise of cGMP. These results suggest the substantial tonic production of NO in the intact CNS and its link to cGMP pathways.

B. We cloned the full length gene of *AcNOS* from the model organism *Aplysia* and mapped nitrergic neurons in its CNS using *in situ* hybridization and immunocytochemistry. A similar pattern of NOS expression was observed with both techniques, with up to 390 nitrergic neurons labeled with NOS selective RNA-probes including several identified neurons, which corresponds to 1-2% of all central neurons. The majority of nitrergic neurons were located in the cerebral (~145) and buccal (~84) ganglia followed by pedal (~41), abdominal (~21) ganglion and pleural (~8) ganglia. A conceptual translation of the *Ac*NOS cloned gene yielded a protein of 1387 amino acid residues. *Ac*NOS is structurally similar to neuronal NOS (NOS-I type in mammals) and contains all of the conserved sites characteristic of a functional NOS.

C. In order to examine the functional implications of NO in nerve regeneration and neuropathic pain, the effect of unilateral pedal nerve crush on the level of expression of NOS mRNA in *Aplysia* pedal neurons was studied in paper C. ISH and densitometry showed that the number of neurons and the intensity of neuronal staining following unilateral pedal nerve crush was significantly reduced in cells on the injured side. In contrast, a significant increase of *Ac*NOS mRNA was detected in pedal nerve axoplasm by RT-PCR within the same timeframe. Complimentary experiments need to be done to confirm the hypothesis whereby the diminished expression pattern of *Ac*NOS mRNA in the soma can be explained by its translocation to the injury site for peripheral translation during adaptive responses to nerve injury.

D. A highly sensitive protocol for double chromophore labeled ISH has been developed and optimized for whole-mount preparations of *Aplysia* CNS. It has been successfully used for *Aplysia* weighing between 10 and 300 g. This procedure can also be used for molecular mapping of expressed genes in combination with electrophysiological mapping of identified neurons. Lucifer Yellow labeling of specific cells following electrophysiology is retained

during ISH, thus the identity of a cell can be positively matched with any particular gene it may express.

E. The presented study adapted and utilized in situ hybridization, staining by nerve back-fill and soma injection, and electrophysiological methods to characterize the locations, numbers, and functions of sensorin-A-expressing neurons and to define the relationships between soma locations and the locations of peripheral axons and receptive fields. Approximately 1,000 cells express sensorin-A mRNA. All of the labeled somata are in the CNS, primarily in the abdominal LE, rLE, RE and RF, pleural VC, cerebral J and K, and buccal S clusters. Together, receptive fields of all these mechanosensory clusters cover the entire body surface. Each VC cluster forms a somatotopic map of the ipsilateral body, a "sensory apluncus." Neurons in all of the clusters appeared to have relatively high mechanosensory thresholds, responding preferentially to threatening or noxious stimuli. Synaptic outputs to target cells having defensive functions support a nociceptive role, as does peripheral sensitization following noxious stimulation, although additional functions are likely in some clusters.

F. We identified and cloned a new heme enzyme from *Aplysia.* a putative thyroid peroxidase (*Aca*TPO). The *Aplysia* peroxidase gene showed high sequence similarity with peroxidasin and thyroid peroxidases, the critical TH synthesis enzymes found in all vertebrates. Data presented in the paper provide evidence for thyroid hormone-related signaling in *Aplysia* and evidence of endogenous TH synthesis. Furthermore, spatial and temporal expression patterns of these transcripts suggest a role of *Aca*TPO in a variety of processes such as developmental metamorphosis and regulation of the animal's energy metabolism.

CHAPTER II.

COPORPHYRINOGEN III OXIDASE (CPO) ENZYME –CLONING, LOCALIZATION OF CPO IN *APLYSIA CALIFORNICA* AND CRYSTALLIZATION OF HUMAN CPO

RESULTS AND DISCUSSION II.

Cloning of the coproporphyrinogen oxidase gene from the cDNA of Aplysia californica.

Several phylogenetically unrelated species from the Gene Bank were chosen that contain the CPO gene, and from this sequence alignment we chose the most conserved parts of CPX gene and designed degenerate primers for this region. CPX_rev CCRAAYTTNGTNCCNCKRTCRTA and CPX_dir : ATHGGNGGNATHTTYTTYGAY

GA were useful in pulling out the *Ap*CPX sequence from the *Aplysia* cDNA. Using the RACE Method (35), designing the nested primers and specific adapter primers ligated at the 3'a 5' ends of the genes in the cDNA library of the CNS of *Aplysia* we obtained the full sequence of *Ap*CPX gene. Sequence was submitted to gene bank and the accession numer is AF51085.1 (CPX, AF510850.1, GI:30515681).

In situ hybridization with antisense RNA probe from the full length clone coproporphyrinogen oxidase from *Aplysia* (*Ap*CPX) was localized in the CNS in the cerebral ganglia in th F cluster of neurons. The F cluster consists of symetrical clusters located in lateral part of each hemiganglion, on the dorsal surface near the cerebral commissure and morphologically distinct neurons in this region appear to be neuroendocrine cells (74).

The analysis of highest BLAST homology (55) of these molluscan CPO sequence reveals the maximum identity of 68% with *Drosophila* and 63% with *Homo sapiens*.

Crystallization of human CPO

The Protein Fold

CPO assumes a previously unknown tertiary topology characterized by a large seven-stranded β-sheet that is flanked on both sides by α-helices (Figure 9*B*). The up-and-down β -strands are similar to porins, but the β-sheet in CPO is flat (Figure 9 B) and does not form a barrel. The flatness of the up-and-down β-sheet in CPO is striking (Figure 9A). In contrast, seven-stranded β -sheet-containing enzymes usually contain a twisted (TauD;(75)) or highly curved (thiol ester dehydrase;(76)) β-sheet whose convex or the apolar concave side, respectively, is flanked by helices. The flatness of the CPO sheet is very likely enabled by the abundance of Gly residues found within the β -strands (β 2, β 3, β 4, β 6, and β 7).

Figure 9. Structure of human CPO. (*A*) Tertiary topology and quaternary structure. (*B*) Topology diagram illustrating the organization of secondary structural elements in human CPO. Filled circles and triangles represent α-helices and β-strands, respectively.

The Active Site

We discovered that an electropositive cleft (Figure 10A) near the dimer interface had a molecule of citrate (Figure 10B) bound to it.

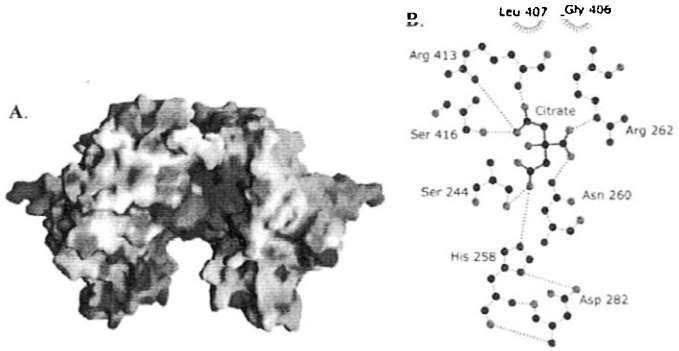

Figure 10. Active site of human CPO. (*A*) Electrostatic potential mapped on to the molecular surface. The electropositive active site cleft is readily visible. The blue and red contours represent positive and negative potential (full saturation = 10 kT), respectively (Figure was generated by using GRASP; (77)). (*B*) Schematic illustration of the amino acid residues that make direct contact with the bound citrate. Dashed lines indicate H bonds, and nonbonded contacts are represented by an arc with spokes radiating toward the ligand atoms (Figure was generated by using LIGPLOT; (78)).

In proteins, arginine residues are hot candidates for carboxylate recognition (79) and by comparing >500 unique sequences of CPO (>350 of these sequences are from the environmental samples of the Sargasso Sea; (80)), we have identified that Arg-262, Arg-328, Arg-332, and Arg-389 are invariant. In addition, there are no conserved Lys residues. Arg-262 forms a key ionic interaction with citrate and Arg-332 is within striking distance. Thus, where coproporphyrinogen III and harderoporphyringen are concerned, we conclude that Arg-262 mediates substrate recognition.

Catalytic Mechanism

CPO catalyzes an unusual metal- and cofactor independent oxidative decarboxylation. It is well established that CPO abstracts the *pro-S* hydrogen from the methylene group adjacent to the pyrrole ring, leading to the generation of a vinyl group from the remaining three hydrogens and two carbons without rearrangement. Such strong stereoselectivity indicates that CPO strictly constrains the orientation of the substrate in the active site, and our structure provides insights into how this result can be achieved (*vide supra*). However, the precise mechanism for hydrogen abstraction is unknown. We favor a mechanism in

which oxygen serves as the immediate electron acceptor, and a substrate radical or a carbanion with substantial radical character participates in catalysis.

Structural Basis of Disease

There are several naturally occurring HCP mutations, in this study we discuss mutations for which meaningful insights can be provided solely by inspecting the structure of the native enzyme. First, deletion of the region encoded by exon six, comprising residues 392–418, has been reported in a heterozygous patient, and the resulting protein will be unable to dimerize. Indeed, we have confirmed this prediction by expressing the variant in *E. coli*. Trp-427, located on strand β8, makes intersubunit interactions, and, therefore, W427R mutation will also affect dimerization. Second, H327R and R328C will perturb the interaction between helix β 7 and the dimerization helix 9. Third, R331W variant retains sufficient activity to support life in a homozygous setting but can also produce HCP in a heterozygote. Twelve different amino acids are tolerated at position 331 but aromatic residues are not. R331W substitution will abolish the hydrogen bonds between the guanidinium group and the carbonyl of Leu-446 and Arg-447. Interestingly, R447C mutation also results in diminished activity. Finally, K404E causes harderoporphyria, a disease with symptoms unrelated to HCP (81-83). In the human CPO structure, K404 is part of a type I β-turn. Whereas a positively charged residue at this position is not essential for the second decarboxylation step, introducing a negative charge will produce electrostatic repulsion (or steric hindrance), and the enzyme will lose its ability to hold on to harderoporphyrinogen.

This study was performed in cooperation with Prof. Moroz's lab at Whitney Laboratory, Saint Augustine, FL, USA and Dr.Raman's lab at the Department of Biochemistry and Molecular Biology, University of Texas Medical School, Houston, TX, USA. My contribution to this study was to identify and clone the coproporphyrinogen oxidase from *Aplysia*, together with data submission to NCBI. Then to localize *Ac*CPO transcript in the CNS of *Aplysia*, perform the phylogenetic analysis, to clone the bacterial CPO from *Chlorophlexus aurantiacus* and *E.coli*, and prepare the CPO expression vectors.

CONCLUSIONS FOR CHAPTER II.

G. The CPO from *Aplysia* has been cloned and we showed its location in the metabolically active part of the CNS of *Aplysia*.

For the first time we report the crystal structure of human CPO at 1.58-Å resolution. The structure reveals a previously uncharacterized tertiary topology comprising an unusually flat seven stranded β-sheet sandwiched by α-helices. Our work has revealed the identity of active site residues in CPO and on the molecular level for several CPO mutations has provided explanation how these alterations diminish enzyme activity for several CPO mutations.

REFERENCES

1. Arnold WP, Mittal CK, Katsuki S, & Murad F (1977) *Proc Natl Acad Sci U S A* 74, 3203-3207.
2. Bredt DS & Snyder SH (1989) *Proc Natl Acad Sci U S A* 86, 9030-9033.
3. Bredt DS & Snyder SH (1990) *Proc Natl Acad Sci U S A* 87, 682-685.
4. Regulski M & Tully T (1995) *Proc Natl Acad Sci U S A* 92, 9072-9076.
5. Elphick MR, Green IC, & O'Shea M (1993) *Brain Res* 619, 344-346.
6. Kone BC, Kuncewicz T, Zhang W, & Yu ZY (2003) *Am J Physiol Renal Physiol* 285, F178-190.
7. Garthwaite J, Charles SL, & Chess-Williams R (1988) *Nature* 336, 385-388.
8. Koh SD, Campbell JD, Carl A, & Sanders KM (1995) *J Physiol* 489 (Pt 3), 735-743.
9. Lynch JW (1998) *J Membr Biol* 165, 227-234.
10. Summers BA, Overholt JL, & Prabhakar NR (1999) *J Neurophysiol* 81, 1449-1457.
11. Lipton SA, Choi YB, Pan ZH, Lei SZ, Chen HS, Sucher NJ, Loscalzo J, Singel DJ, & Stamler JS (1993) *Nature* 364, 626-632.
12. Stamler JS, Simon DI, Osborne JA, Mullins ME, Jaraki O, Michel T, Singel DJ, & Loscalzo J (1992) *Proc Natl Acad Sci U S A* 89, 444-448.
13. Savchenko A, Barnes S, & Kramer RH (1997) *Nature* 390, 694-698.
14. Huang Z, Huang PL, Panahian N, Dalkara T, Fishman MC, & Moskowitz MA (1994) *Science* 265, 1883-1885.
15. Okere CO & Kaba H (2000) *Eur J Neurosci* 12, 4552-4556.
16. Wu HH, Williams CV, & McLoon SC (1994) *Science* 265, 1593-1596.
17. Cudeiro J & Rivadulla C (1999) *Trends Neurosci* 22, 109-116.
18. Calapai G, Squadrito F, Altavilla D, Zingarelli B, Campo GM, Cilia M, & Caputi AP (1992) *Neuropharmacology* 31, 761-764.
19. Watanabe A, Ono M, Shibata S, & Watanabe S (1995) *Neurosci Lett* 192, 25-28.
20. Mao J (1999) *Brain Res Brain Res Rev* 30, 289-304.
21. Zheng YM, Schafer MK, Weihe E, Sheng H, Corisdeo S, Fu ZF, Koprowski H, & Dietzschold B (1993) *J Virol* 67, 5786-5791.
22. Adamson DC, Wildemann B, Sasaki M, Glass JD, McArthur JC, Christov VI, Dawson TM, & Dawson VL (1996) *Science* 274, 1917-1921.
23. Lovell P & Moroz LL (2006) *Integr. Comp. Biol.* 46, 847-870.
24. Kandel ER (2001) *Science* 294, 1030-1038.
25. Sharma SK & Carew TJ (2004) *Learn Mem* 11, 373-378.
26. Teyke T, Weiss KR, & Kupfermann I (1991) *Neurosci Lett* 133, 307-310.
27. Proekt A & Weiss KR (2003) *J Neurosci* 23, 4029-4033.
28. Proekt A, Brezina V, & Weiss KR (2004) *Proc Natl Acad Sci U S A* 101, 9447-9452.
29. Bedi SS & Glanzman DL (2001) *J Neurosci* 21, 9667-9677.
30. Weragoda RM, Ferrer E, & Walters ET (2004) *J Neurosci* 24, 10393-10401.
31. Cropper EC, Evans CG, Jing J, Klein A, Proekt A, Romero A, & Rosen SC (2004) *Acta Biol Hung* 55, 211-220.
32. Moroz LL, Edwards JR, Puthanveettil SV, Kohn AB, Ha T, Heyland A, Knudsen B, Sahni A, Yu F, Liu L, *et al* (2006) *Cell* 127, 1453-1467.
33. Matz MV (2002) *Methods Mol Biol* 183, 3-18.
34. Kacharmina JE, Crino PB, & Eberwine J (1999) *Methods Enzymol* 303, 3-18.
35. Matz MV, Alieva NO, Chenchik A, & Lukyanov S (2003) *Methods Mol Biol* 221, 41-49.
36. Bogdanov Yu D, Balaban PM, Zakharov IS, Poteryaev DA, & Belyavsky AV (1996) *Invert Neurosci* 2, 61-69.
37. Jezzini SH, Bodnarova M, & Moroz LL (2005) *Journal of Neuroscience Methods* 149, 15-25.
38. Beavo JA, Hardman JG, & Sutherland EW (1970) *J Biol Chem* 245, 5649-5655.
39. Garthwaite J, Southam E, Boulton CL, Nielsen EB, Schmidt K, & Mayer B (1995) *Mol Pharmacol* 48, 184-188.
40. Morley D, Maragos CM, Zhang XY, Boignon M, Wink DA, & Keefer LK (1993) *J Cardiovasc Pharmacol* 21, 670-676.
41. Huang S, Kerschbaum HH, & Hermann A (1998) *Brain Res* 780, 329-336.
42. Laemmli UK (1970) *Nature* 227, 680-685.
43. Towbin H, Staehelin T, & Gordon J (1979) *Proc Natl Acad Sci U S A* 76, 4350-4354.
44. Walters ET, Alizadeh H, & Castro GA (1991) *Science* 253, 797-799.

45. Thompson JD, Gibson TJ, Plewniak F, Jeanmougin F, & Higgins DG (1997) *Nucleic Acids Res* 25, 4876-4882.
46. Martasek P, Camadro JM, Raman CS, Lecomte MC, Le Caer JP, Demeler B, Grandchamp B, & Labbe P (1997) *Cell Mol Biol (Noisy-le-grand)* 43, 47-58.
47. Koh HY & Jacklet JW (1999) *J Neurosci* 19, 3818-3826.
48. Elofsson R, Carlberg M, Moroz L, Nezlin L, & Sakharov D (1993) *Neuroreport* 4, 279-282.
49. Stuehr DJ & Griffith OW (1992) *Adv Enzymol Relat Areas Mol Biol* 65, 287-346.
50. Huang S, Kerschbaum HH, Engel E, & Hermann A (1997) *J Neurochem* 69, 2516-2528.
51. Luo D, Leung E, & Vincent SR (1994) *J Neurosci* 14, 263-271.
52. Aonuma H (2002) *Zoolog Sci* 19, 969-979.
53. Koh HY & Jacklet JW (2001) *Eur J Neurosci* 13, 553-560.
54. Fujie S, Aonuma H, Ito I, Gelperin A, & Ito E (2002) *Zoolog Sci* 19, 15-26.
55. Altschul SF, Gish W, Miller W, Myers EW, & Lipman DJ (1990) *J Mol Biol* 215, 403-410.
56. Moroz LL (2006) *J Comp Neurol* 495, 10-20.
57. Antonov I, Ha T, Antonova I, Moroz LL, & Hawkins RD (2007) *J Neurosci* 27, 10993-11002.
58. McAllister LB, Scheller RH, Kandel ER, & Axel R (1983) *Science* 222, 800-808.
59. Ono JK & McCaman RE (1992) *J Neurosci Methods* 44, 71-79.
60. Levenson J, Sherry DM, Dryer L, Chin J, Byrne JH, & Eskin A (2000) *J Comp Neurol* 423, 121-131.
61. Moccia R, Chen D, Lyles V, Kapuya E, E Y, Kalachikov S, Spahn CM, Frank J, Kandel ER, Barad M, *et al.* (2003) *J Neurosci* 23, 9409-9417.
62. Brunet JF, Shapiro E, Foster SA, Kandel ER, & Iino Y (1991) *Science* 252, 856-859.
63. Price DA & Greenberg MJ (1977) *Prep Biochem* 7, 261-281.
64. Bastiani MJ, Harrelson AL, Snow PM, & Goodman CS (1987) *Cell* 48, 745-755.
65. Vilim FS, Alexeeva V, Moroz LL, Li L, Moroz TP, Sweedler JV, & Weiss KR (2001) *Peptides* 22, 2027-2038.
66. Jezzini SH & Moroz LL (2004) *Brain Res Mol Brain Res* 127, 27-38.
67. Walters ET, Bodnarova M, Billy AJ, Dulin MF, Diaz-Rios M, Miller MW, & Moroz LL (2004) *J Comp Neurol* 471, 219-240.
68. Cash D & Carew TJ (1989) *J Neurobiol* 20, 25-47.
69. Byrne J, Castellucci V, & Kandel ER (1974) *J Neurophysiol* 37, 1041-1064.
70. Dubuc B & Castellucci VF (1991) *J Exp Biol* 156, 315-334.
71. Walters ET, Byrne JH, Carew TJ, & Kandel ER (1983) *J Neurophysiol* 50, 1522-1542.
72. Rosen SC, Weiss KR, & Kupfermann I (1979) *J Neurophysiol* 42, 954-974.
73. Fiore L & Geppetti L (1985) *Behav Brain Res* 16, 37-45.
74. Rubakhin SS, Li L, Moroz TP, & Sweedler JV (1999) *J Neurophysiol* 81, 1251-1260.
75. O'Brien JR, Schuller DJ, Yang VS, Dillard BD, & Lanzilotta WN (2003) *Biochemistry* 42, 5547-5554.
76. Leesong M, Henderson BS, Gillig JR, Schwab JM, & Smith JL (1996) *Structure* 4, 253-264.
77. Nicholls A, Sharp KA, & Honig B (1991) *Proteins* 11, 281-296.
78. Wallace AC, Laskowski RA, & Thornton JM (1995) *Protein Eng* 8, 127-134.
79. Raman CS, Martasek P, & Masters BS (2000) in *The Porphyrin Handbook* (Academic, N.Y.), pp. 293-339.
80. Venter JC, Remington K, Heidelberg JF, Halpern AL, Rusch D, Eisen JA, Wu D, Paulsen I, Nelson KE, Nelson W, *et al.* (2004) *Science* 304, 66-74.
81. Lamoril J, Puy H, Whatley SD, Martin C, Woolf JR, Da Silva V, Deybach JC, & Elder GH (2001) *Am J Hum Genet* 68, 1130-1138.
82. Nordmann Y, Grandchamp B, de Verneuil H, Phung L, Cartigny B, & Fontaine G (1983) *J Clin Invest* 72, 1139-1149.
83. Lamoril J, Martasek P, Deybach JC, Da Silva V, Grandchamp B, & Nordmann Y (1995) *Hum Mol Genet* 4, 275-278.

LIST OF ORIGINAL COMMUNICATIONS

This thesis is based on the following publications, which will be referred to in the text by capital letters (A-G). Impact Factors (IF) and citation frequency as at May 2008 are shown.

A. **Bodnárová M**, Martásek P, Moroz LL : Calcium/calmodulin-dependent nitric oxide synthase activity in the CNS of *Aplysia californica*: Biochemical characterization and link to cGMP pathways. J Inorg Biochem. 2005;99(4):922-8. IF= 2.423, 6 citations

B. Moroz LL, **Buganová M**, Sadreev R, Uvarov P, Martásek P, Panchin Yu: Cloning and localization of nitric oxide synthase in the CNS of *Aplysia californica*. (manuscript in preparation).

C. **Buganová M**, Sung Y-J, Ambron RT , Walters ET, Moroz LL: Nerve injury in *Aplysia* reduces nitric oxide synthase mRNA levels in neuronal somata while increasing mRNA levels in axoplasm. (Program No. 497.11. *2004 Abstract Viewer*. Washington, DC: Society for Neuroscience, 2004. Online.)

D. Jezzini SH*, **Bodnárová M***, Moroz LL: Two-color in situ hybridization in the CNS of *Aplysia californica*. J Neurosci Methods. 2005;149(1):15-25. *authors contributed equally to the publication, IF= 1.784, 7 citations

E. Walters ET, **Bodnárová M**, Billy AJ, Dulin MF, Diaz-Rios M, Muller M, Moroz LL: Somatotopic organization and functional properties of mechanosensory neurons expressing sensorin-A mRNA in *Aplysia* californica. J Comp Neurol. 2004 Mar 29;471(2):219-40. IF= 2.200, 14 citations

F. Heyland A, Price DA, **Bodnárová M**, Moroz LL.: Thyroid hormone metabolism and peroxidase function in two non-chordate animals. J Exp Zoolog B Mol Dev Evol. 2006 May 31. IF= 2.756, 1 citation

G. Lee DS, Flachsová E, **Bodnárová M**, Demeler B, Martásek P, Raman CS.: Structural basis of hereditary coproporphyria. Proc Natl Acad Sci U S A. 2005 Oct 4;102(40):14232-7. IF= 10.231, 8 citations